Chemical Physics Letters 739 (2020) 136999

Contents lists available at ScienceDirect

Chemical Physics Letters

journal homepage: www.elsevier.com/locate/cplett

Research paper

Hydrophobic agglomeration of montmorillonite fines in aqueous solutions induced by dodecyl trimethyl ammonium bromides

Weiquan Zhan[a], Yuan Yuan[b], Hao Yi[b], Shaoxian Song[a,*], Cheng Liu[b,*]

[a] Hubei Key Laboratory of Mineral Resources Processing and Environment, Wuhan University of Technology, Luoshi Road 122, Wuhan, Hubei 430070, China
[b] School of Resources and Environmental Engineering, Wuhan University of Technology, Luoshi Road 122, Wuhan, Hubei 430070, China

HIGHLIGHTS

- Hydrophobic agglomeration behaviors of montmorillonite are firstly studied.
- DTAB is used for masking the hydrophilic sites of montmorillonite.
- Adsorbed DTAB tails together with siloxane site greatly increase hydrophobic agglomeration of montmorillonite.

ARTICLE INFO

Keywords:
Hydrophobic agglomeration
Montmorillonite
Aggregation degree
DTAB

ABSTRACT

Dodecyl trimethyl ammonium bromides (DTAB) was used to adsorb on the isomorphous substitutions of montmorillonite (MMT) for masking hydrophilic sites. The adsorbed DTAB tails together with siloxane sites of MMT surfaces would greatly increase hydrophobicity of MMT, leading to stronger hydrophobic agglomeration of MMT fines in water. The experimental results showed that DTAB was adsorbed on the isomorphous substitution sites of MMT due to electrostatic interaction, and thus rendered MMT surfaces more hydrophobic. The aggregation of MMT fines in water was greatly enhanced by the addition of DTAB because of the formation of hydrophobic agglomeration at an appropriate shear field.

1. Introduction

Recently, montmorillonite (MMT) had numerous applications such as adsorbents [1], catalysts [2] and pharmaceuticals [3] owing to its colloidal, electrical, thermal stability and adsorption properties. However, MMT with strong hydrophilicity [4] was hard to be recycled from aqueous solutions, which would be detrimental to its actual industrial applications. In environmental fields, MMT was difficultly separated from aqueous solutions after adsorption of pollutants [5]. In mineral processing, super wettability of MMT caused a poor flotation separation performance, leading to a detrimental effect on flotation recovery [6]. As for composite materials, hydrophilicity of MMT had adverse impact on the efficient recycling from water resource [7–9]. Thus, separating MMT from water was quite important in various industrial processes.

To realize the solid-liquid separation, aggregation was an indispensable step during the process [10]. Among many aggregation methods, hydrophobic agglomeration caught wide attractions because large and compact flocs could be gained for solving the problems in concentrating and dewatering process [11–13]. Hydrophobic agglomeration occurred from strong hydrophobic attractive forces between particles in aqueous solutions [14]. Generally speaking, surfactants were applied for rendering mineral more strong hydrophobicity so that enhancing the sizes of flocs [15,16]. For instance, dodecylamine was used for inducing strong aggregation of colloidal kaolinite fines [17]. The effect of dodecylamine hydrochloride on hydrophobic agglomeration of graphene oxide had been studied [18]. Also, Loosli et al. [19] investigated the effect of surfactants on the surface properties and agglomeration behavior of TiO_2 nanoparticles. However, few investigations had reported the hydrophobic agglomeration of MMT fines in aqueous solutions.

MMT, a layered aluminosilicate mineral with 2:1 structural cell consisted of two layers of silica tetrahedron (siloxane) sandwiched one layer of alumina octahedral, had received extensive attentions worldwide [20–22]. Isomorphous substitutions of crystal structure of MMT were ubiquitous in natural state, for example, substitution of Al^{3+} in octahedral sites by Mg^{2+} and Si^{4+} by Al^{3+} in tetrahedral sites, producing a negative surface charge sites [23]. Balanced exchangeable cations such as Na^+, K^+ and Ca^{2+} were absorbed on the isomorphous

* Corresponding authors.
E-mail addresses: ssx851215@whut.edu.cn (S. Song), 145601011@csu.edu.cn (C. Liu).

https://doi.org/10.1016/j.cplett.2019.136999
Received 25 October 2019; Received in revised form 21 November 2019; Accepted 27 November 2019
Available online 28 November 2019
0009-2614/

substitution sites, which had strong tendency to hydrate [24]. Considering that the hydrophobic property of Siloxane structure, hydrophilicity of MMT mainly originated from hydration of exchangeable ions [25]. Therefore, cationic surfactant was used to mask the isomorphous substitution sites for exposing the siloxane structure, achieving hydrophobic agglomeration of MMT.

In this work, hydrophobic agglomeration of MMT fines in aqueous solutions in the presence of dodecyl trimethyl ammonium bromides (DTAB) as well as the interaction mechanism would be studied. In-situ turbidity measurement was performed on studying the hydrophobic agglomeration behaviors of DTAB modified MMT. The mechanism was researched by X-ray diffraction (XRD), Fourier Transform Infrared Spectroscopy (FTIR) and Zeta potential. The aims of the work were to further understand the hydrophobic agglomeration of MMT in aqueous suspensions, and to suggest a pathway for improving the removal of MMT in industrial products.

2. Experimental

2.1. Materials

The original MMT sample was obtained from Chifeng Ningcheng Montmorillonite Co., Ltd, Inner Mongolia, China. Purified MMT was acquired by centrifuging original MMT by a Sorvall St16 centrifuge (Thermo Fisher Scientific, U.S.A.) to remove sedimentation impurities. Cumulative particle size distribution of MMT fines was determined by Malvern Mastersizer 2000, and exhibited in Fig. 1. The results revealed that the d_{50} and d_{90} of MMT size were of 1.96 μm and 4.95 μm, respectively, indicating MMT belonged to fine particle level.

DTAB was analytical purity from Sinopharm Chemical Reagent Co., Ltd (China). The water with 18.2 MΩ used in the whole experiment was ultra-pure water produced by a Milli-Q Direct 8/16 water purification system.

2.2. Tests on hydrophobic agglomeration of MMT

Hydrophobic agglomeration tests of MMT was performed in a tank described in our previous works [11]. MMT suspension (0.5% concentration) was strongly agitated at certain stirring speed in the presence of DTAB.

The relation between turbidity of flocs suspension and time was attained to match specific function, and the equation was showed below:

$$\ln(y - y_0) = \ln A_0 - \frac{x}{t_1} \tag{1}$$

where y meant the turbidity of MMT flocs suspension; x denoted the time of sedimentation; and y_0 and t_1 were the corresponding constants.

Average sizes of flocs were evaluated by the slope K of Eq. (1), which was expressed as:

$$\mathrm{K} = \frac{1}{t_1} \tag{2}$$

Agglomeration degree E of MMT fines was defined as:

$$\mathrm{E} = \frac{T_0 - T_E}{T_0} \times 100 \tag{3}$$

where T_0 and T_E meant the beginning and final turbidity of the flocs suspension, respectively.

2.3. DTAB adsorption capacity measurements

The residual concentration of DTAB was detected. In step 1, 5 mL suspension was filtered with 0.22 μm filter membrane. In step 2, first 2 mL was discarded and another 3 mL was leaved for analysis. In step 3, the concentration of DTAB solution was diluted less than 5 mg/L. In step 4, the absorbance of DTAB was measured using a UV spectrophotometer at the wavelength of 198 nm. Finally, the concentration of DTAB in solution was calculated according to the standard line (Fig. 2).

DTAB adsorption capacity was calculated through the following equation:

$$q = \frac{V_0 C_0 - CV}{m} \tag{4}$$

where q (mg/g) meant the adsorption capacity of adsorbent (MMT); C_0 and C (mg/L) were the DTAB concentration in the suspension before and after adsorption, respectively; V_0 and V exhibited the solution volume of DTAB solution before and after adsorption, respectively, L; m revealed the mass of the adsorbent in the test, g.

2.4. Characterization

XRD patterns of purified MMT and MMT modified by DTAB were obtained by D8 Advance X-ray diffract meter. Morphology and the energy dispersive spectra (EDS) of MMT modified with DTAB samples were observed using JSM-7100 scanning electron microscope (SEM). FTIR spectrum of MMT before and after modification by DTAB were determined by a Nexus FTIR spectrometer (Thermo Nicolet, US) for characterizing the interaction between MMT and DTAB. The Zeta potentials of MMT suspension in the presence of various DTAB concentration was detected by Zetasizer Zeta-nano.

The measurement of contact angle: MMT suspension in the presence

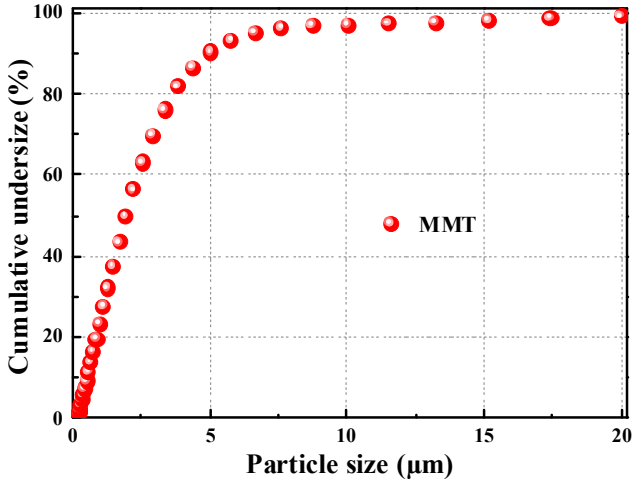

Fig. 1. Size distribution of MMT sample.

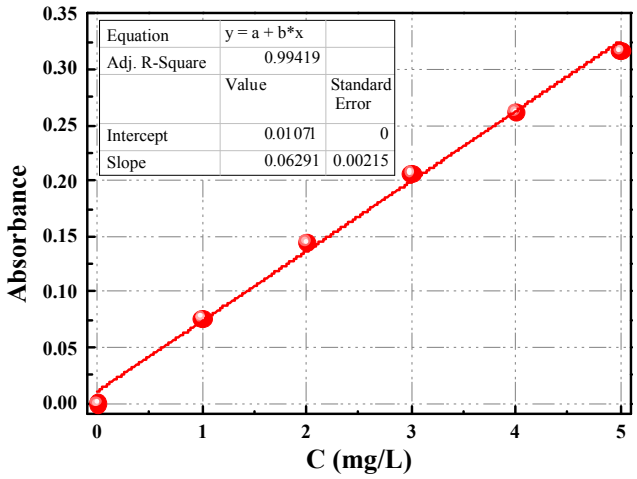

Fig. 2. Standard line of relation between DTAB concentration and absorbance.

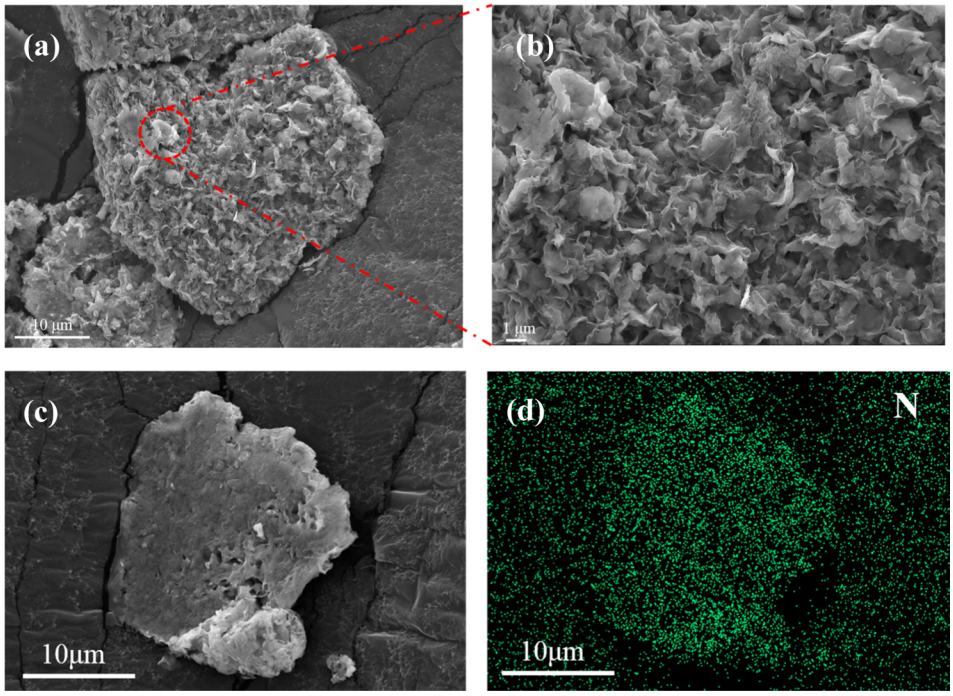

Fig. 3. SEM images (a–c) and corresponding EDS mapping (d) of MMT modified with DTAB.

of various DTAB dosages was dried through freezing, and then ground to power. Follow on, about 1 g MMT powder was made into disc with 5 mm thick at 18 MPa. Finally, contact angle of MMT in the presence of different concentration of DTAB was measured with JC2000DM contact angle measurement.

3. Results and discussion

3.1. Interaction mechanism between DTAB and MMT

SEM was used for characterizing the morphology of MMT modified by DTAB in dry state. As Fig. 3 outlined, MMT modified with DTAB exhibited a dense and aggregate structure. Meanwhile, the homogeneous distribution of the nitrogen element on MMT (Fig. 3d) meant the good adsorption of DTAB on the surface of MMT. XRD results of MMT modified by DTAB before and after were exhibited in Fig. 4. The peaks of MMT with and without DTAB were similar, indicating no DTAB interacted with MMT in the interlayer. Therefore, DTAB combined with MMT on the surface. FTIR was carried out for further

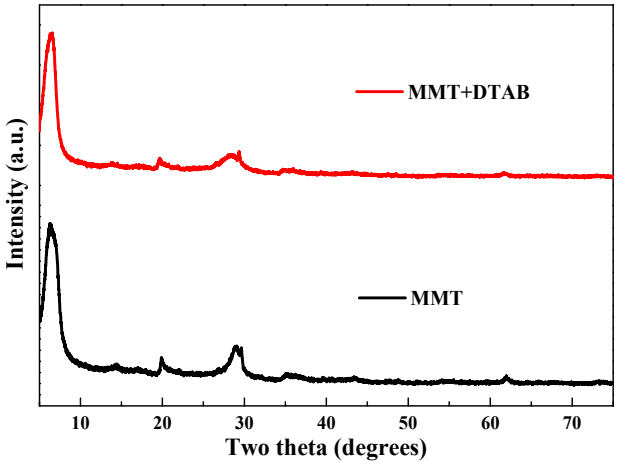

Fig. 4. XRD patterns of MMT and MMT modified by DTAB.

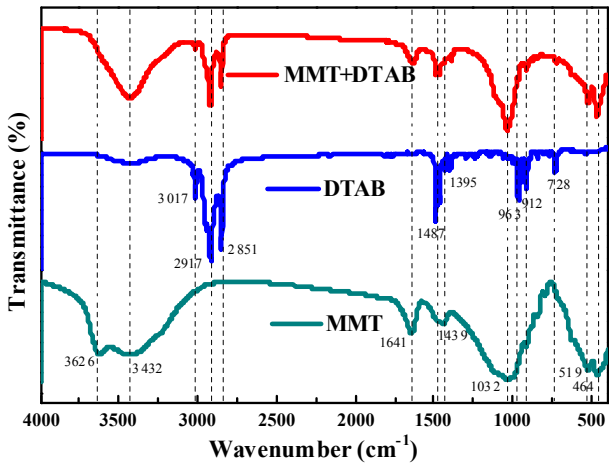

Fig. 5. FTIR curves of MMT, DTAB and DTAB modified MMT.

researching the interaction between MMT and DTAB as shown in Fig. 5. As seen, typical vibrations of Si-O-Si at 1032 cm^{-1} and 464 cm^{-1} were ascribed to MMT [26,27]. With regard to DTAB, characteristic peak at 3017 cm^{-1} originated from CH_3-N^+ vibration and the peaks at 963 and 912 cm^{-1} were correspond to C-N stretching vibration [28–30]. In the spectrum of MMT modified by DTAB, all the primary peaks of MMT and DTAB appeared, demonstrating the combination between MMT and DTAB. The peaks at 963 and 912 cm^{-1} of DTAB were no obvious in the final composition might owing to the effect of high intensity vibration at 1032 cm^{-1} of MMT. Besides, no appeared new peaks indicated the combination without chemical interaction. Then, in Fig. 6, zeta potential of MMT in various concentration of DTAB was detected. With the concentration of DTAB increasing, zeta potential of MMT sharply increased at first and then toward to flat. It revealed that the interaction between MMT and DTAB was mainly through electrostatic interaction. The electrostatic adsorption might arise from positively charged DTAB adsorbed at substitution sites of MMT. Afterwards, active sites on surface would be saturated which led to equilibrated interaction between MMT and DTAB. Thus, DTAB could cover the hydrophilic sites of MMT

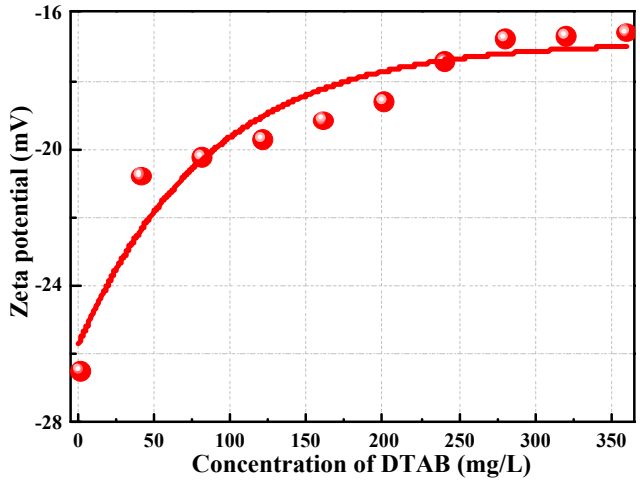

Fig. 6. Zeta potential of MMT with different concentration of DTAB.

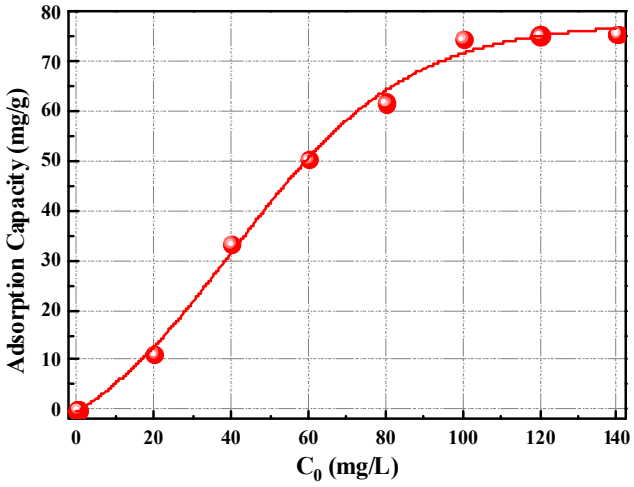

Fig. 8. Adsorption capacity of DTAB on MMT at different initial concentration.

through electrostatic interaction, resulting in the exposure of hydrophobic siloxane structure.

3.2. Hydrophobization of MMT

Contact angle was used for evaluating the hydrophobicity of MMT in the presence of various DTAB concentration, and the results were presented in Fig. 7. The contact angle of MMT sharply increased from 6° to 64° with the concentration from 0 to 80 mg/L of DTAB. After that, the contact angle slowly increased and then reached an equilibrium about 74°. The results indicated that the addition of DTAB could cover the hydrophilic sites thus to realize the hydrophobization of MMT. Accordingly, the adsorption capacity of DTAB on MMT was calculated at different initial concentration, which was exhibited in Fig. 8. It was found that the adsorption capacity increased quickly as the increase of initial DTAB concentration from 0 to 100 mg/L and then reached a

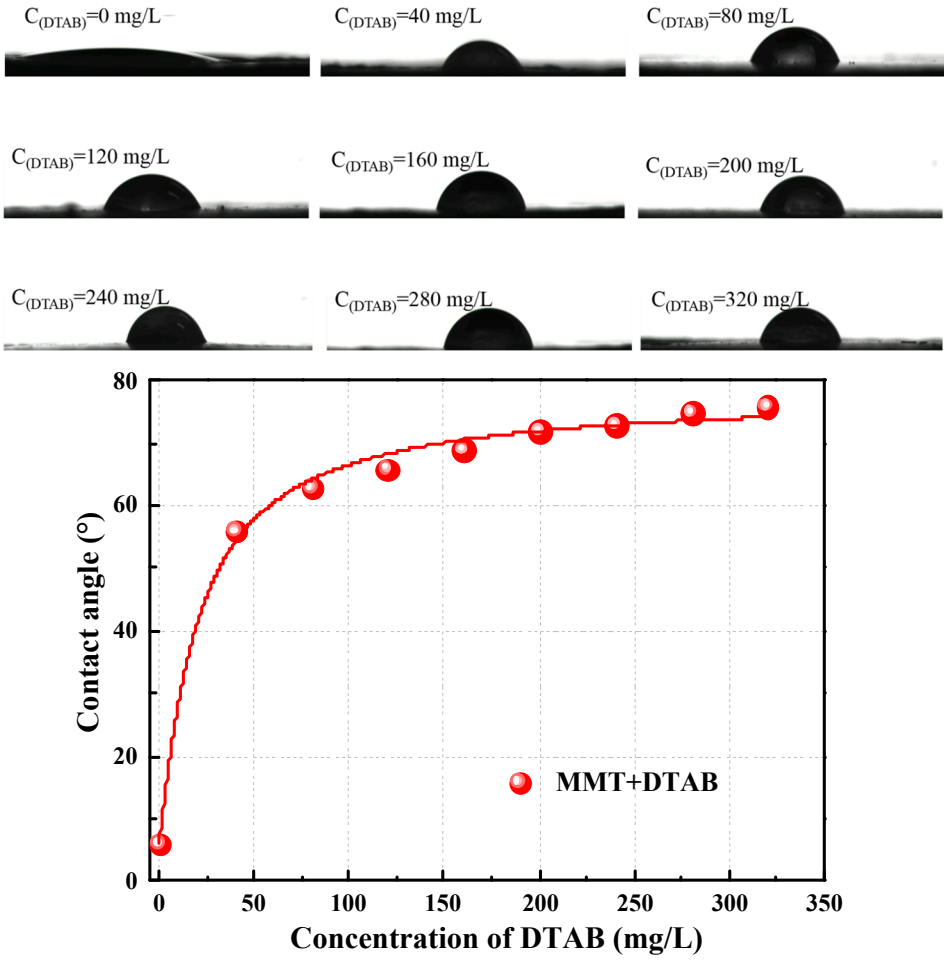

Fig. 7. Photograph (a) and value (b) of contact angle of MMT modified with different DTAB concentration.

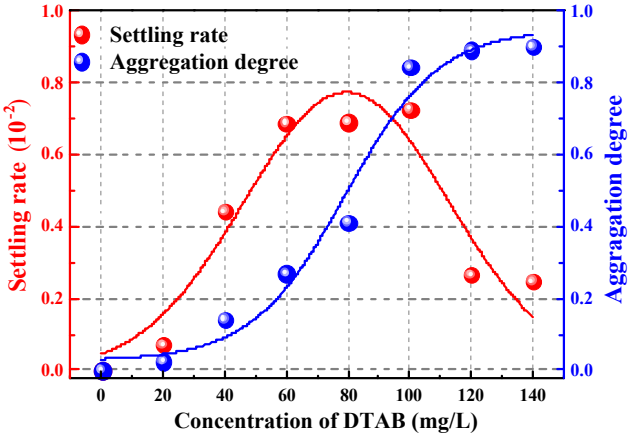

Fig. 9. Impact of DTAB on settling rate and aggregation degree.

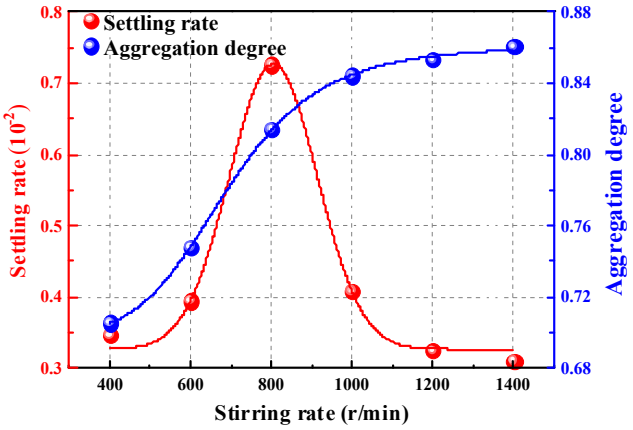

Fig. 10. Impact of stirring rate on settling rate and aggregation degree.

plateau. The efficient adsorption of DTAB on MMT might be highly related with the substitution sites of MMT. Hydrophobization of MMT could achieve through covering the substitution sites so that exposing the siloxane structure.

3.3. Hydrophobic agglomeration of MMT fines

3.3.1. Effect of DTAB concentration

Turbidity of MMT suspension as a function of settling time during sedimentary process at various concentration of DTAB was detected. For illustrating the impact of DTAB concentration on hydrophobic agglomeration of MMT suspension, settling rate and aggregation degree were calculated according to Eqs. (2) - (3), as shown in Fig. 9. It was clear that settling rate increased at first, then achieved maximum value, finally decreased. There may be existed strong hydrophobic force between DTAB adsorbed MMT particles in aqueous solutions, which enabled particles gather together to form flocs. More dosage of DTAB led to stronger hydrophobic of MMT. As a result, larger flocs would come into being with increased addition of DTAB, promoting quicker settling rate owing to gravity. After flocs of MMT reached most stabilized state, flocs would fragile to be broken, resulting in decrease of settling rate. With regard to aggregation degree, it increased and then nearly keep constant. More DTAB was used lead to more MMT particles aggregated to flocs. Hence, DTAB modified MMT could well aggregate to large flocs.

3.3.2. Effect of stirring rate

Mechanical agitation was necessary to endow DTAB modified MMT particles enough kinetics for overcoming energy barrier to realize hydrophobic agglomeration. Thus, the effect of stirring rate on turbidity of DTAB modified MMT was considered. Settling rate and aggregation degree were calculated and exhibited in Fig. 10. With increase of stirring rate, it was visibly that settling rate increased and then followed by a decline. It was well known that no enough kinetic energy to overcome energy barrier under low stirring rate, while flocs would be destructed at high shearing rate [31,32]. Due to equilibrium between flocs formation and disruption, the maximum agglomeration degree existed under medium stirring rate. As for aggregation degree, it increased initially and attained plateau later. The phenomenon would be ascribed to more MMT fines formed into flocs as increase of stirring rate. Then almost all MMT fines agglomerated into flocs, leaving little part of particles dispersed in suspension, resulting in the equilibrium of aggregation degree. Therefore, aggregation behavior of DTAB modified MMT could be affected by stirring rate: large flocs formed under medium stirring rate while less MMT particles dispersed in suspension in high stirring rate.

4. Conclusions

(1) DTAB was adsorbed at the isomorphous substitution sites of MMT due to electrostatic interaction.
(2) The adsorbed DTAB together with siloxane sites of MMT surface lead to strong hydrophobic agglomeration of MMT fines in aqueous solutions.
(3) More hydrophobization of MMT could generate stronger hydrophobic agglomeration degrees.
(4) Appropriate stirring rate provided powerful agglomeration of DTAB modified MMT.

CRediT authorship contribution statement

Weiquan Zhan: Writing - original draft, Writing - review & editing. **Yuan Yuan:** Methodology, Investigation. **Hao Yi:** Supervision. **Shaoxian Song:** Conceptualization, Data curation. **Cheng Liu:** Formal analysis, Validation.

Declaration of Competing Interest

The authors declare that they have no known competing financial interests or personal relationships that could have appeared to influence the work reported in this paper.

Acknowledgements

The financial supports to this work from the National Natural Science Foundation of China (No. 51704212, 51704220 and 51674183), the Natural Science Foundation of Hubei Province (No. 2016CFA013), and the Research Fund Program of Key Laboratory of Rare Mineral, Ministry of Land and Resources (KLRM-KF201802) are gratefully acknowledged.

References

[1] S. Kang, Y. Zhao, W. Wang, T. Zhang, T. Chen, H. Yi, F. Rao, S. Song, Removal of methylene blue from water with montmorillonite nanosheets/chitosan hydrogels as adsorbent, Appl. Surf. Sci. 448 (2018) 203–211, https://doi.org/10.1016/j.apsusc.2018.04.037.
[2] W. Zhou, W. Guan, C. Lu, Natural montmorillonite nanosheet colloid-catalyzed hydrogen peroxide ultra-weak chemiluminescence, RSC Adv. 4 (2014) 15377–15380, https://doi.org/10.1039/c4ra00636d.
[3] S. Tian, J. Li, Q. Tao, Y. Zhao, Z. Lv, F. Yang, H. Duan, Y. Chen, Q. Zhou, D. Hou, Controlled drug delivery for glaucoma therapy using montmorillonite/Eudragit microspheres as an ion-exchange carrier, Int. J. Nanomed. 13 (2018) 415–428, https://doi.org/10.2147/IJN.S146346.
[4] T. Chen, Y. Zhao, S. Song, Correlation of electrophoretic mobility with exfoliation of montmorillonite platelets in aqueous solutions, Colloids Surf. A Physicochem. Eng. Asp. 525 (2017) 1–6, https://doi.org/10.1016/j.colsurfa.2017.04.057.
[5] W. Wang, Y. Zhao, H. Yi, T. Chen, S. Kang, H. Li, S. Song, Preparation and

characterization of self-assembly hydrogels with exfoliated montmorillonite nanosheets and chitosan, Nanotechnology 29 (2018) 1–11.
[6] Y. Xing, X. Xu, X. Gui, Y. Cao, M. Xu, Effect of kaolinite and montmorillonite on fine coal flotation, Fuel 195 (2017) 284–289, https://doi.org/10.1016/j.fuel.2017.01.058.
[7] H. Yi, W. Zhan, Y. Zhao, S. Qu, W. Wang, P. Chen, S. Song, A novel core-shell structural montmorillonite nanosheets/stearic acid composite PCM for great promotion of thermal energy storage properties, Sol. Energy Mater. Sol. Cells. 192 (2019) 57–64 https://linkinghub.elsevier.com/retrieve/pii/S0927024818305816.
[8] K. Peng, L. Fu, J. Ouyang, H. Yang, Emerging parallel dual 2D composites: natural clay mineral hybridizing MoS_2 and interfacial structure, Adv. Funct. Mater. 26 (2016) 2666–2675, https://doi.org/10.1002/adfm.201504942.
[9] X. Zhang, H. Yi, H. Bai, Y. Zhao, F. Min, S. Song, Correlation of montmorillonite exfoliation with interlayer cations in the preparation of two-dimensional nanosheets, RSC Adv. 7 (2017) 41471–41478, https://doi.org/10.1039/c7ra07816a.
[10] W. Li, L. Zhou, Y. Han, Y. Zhu, Y. Li, Effect of carboxymethyl starch on fine-grained hematite recovery by high-intensity magnetic separation: experimental investigation and theoretical analysis, Powder Technol. 343 (2019) 270–278, https://doi.org/10.1016/j.powtec.2018.11.024.
[11] W. Zhan, H. Yi, S. Song, Y. Zhao, F. Rao, Hydrophobic agglomeration behaviors of clay minerals as affected by siloxane structure, Colloids Surf. A. 568 (2019) 36–42, https://doi.org/10.1016/j.colsurfa.2019.01.061.
[12] H. Yi, Y. Zhao, S. Song, Hydrophobic agglomeration kinetics of fine kaolinite particles in aqueous suspensions, J. Dispers. Sci. Technol. 38 (2017) 1336–1341, https://doi.org/10.1080/01932691.2016.1237366.
[13] H. Yi, Y. Zhao, F. Rao, S. Song, Hydrophobic agglomeration of talc fines in aqueous suspensions, Colloids Surf. A Physicochem. Eng. Asp. 538 (2018) 327–332, https://doi.org/10.1016/j.colsurfa.2017.11.017.
[14] B. Yang, S. Song, A. Lopez-Valdivieso, Morphology of hydrophobic agglomerates of molybdenite fines in aqueous suspensions, Sep. Sci. Technol. 50 (2015) 1560–1564, https://doi.org/10.1080/01496395.2014.975365.
[15] H. Yi, X. Zhang, Y. Liu, S. Song, AFM study on the wettability of mica and graphite modified with surfactant DTAB, J. Dispers. Sci. Technol. 39 (2018) 1060–1064, https://doi.org/10.1080/01932691.2017.1381918.
[16] C. Liu, W. Zhang, S. Song, H. Li, A novel method to improve carboxymethyl cellulose performance in the flotation of talc, Miner. Eng. 131 (2019) 23–27, https://doi.org/10.1016/j.mineng.2018.11.003.
[17] Y. Hu, L. Liu, F. Min, M. Zhang, S. Song, Hydrophobic agglomeration of colloidal kaolinite in aqueous suspensions with dodecylamine, Colloids Surf. A Physicochem. Eng. Asp. 434 (2013) 281–286, https://doi.org/10.1016/j.colsurfa.2013.05.074.
[18] P. Chen, H. Li, H. Yi, F. Jia, L. Yang, S. Song, Removal of graphene oxide from water by floc-flotation, Sep. Purif. Technol. 202 (2018) 27–33, https://doi.org/10.1016/j.seppur.2018.03.034.
[19] F. Loosli, S. Stoll, Effect of surfactants, pH and water hardness on the surface properties and agglomeration behavior of engineered TiO_2 nanoparticles, Environ. Sci. Nano. 4 (2017) 203–211, https://doi.org/10.1039/c6en00339g.
[20] T. Chen, Y. Yuan, Y. Zhao, F. Rao, S. Song, Effect of layer charges on exfoliation of montmorillonite in aqueous solutions, Colloids Surf. A Physicochem. Eng. Asp. 548 (2018) 92–97, https://doi.org/10.1016/j.colsurfa.2018.03.066.
[21] R. Guégan, E. Veron, L. Le Forestier, M. Ogawa, S. Cadars, Structure and dynamics of nonionic surfactant aggregates in layered materials, Langmuir 33 (2017) 9759–9771, https://doi.org/10.1021/acs.langmuir.7b01831.
[22] F. Piscitelli, P. Posocco, R. Toth, M. Fermeglia, S. Pricl, G. Mensitieri, M. Lavorgna, Sodium montmorillonite silylation: unexpected effect of the aminosilane chain length, J. Colloid Interface Sci. 351 (2010) 108–115, https://doi.org/10.1016/j.jcis.2010.07.059.
[23] X. Zhang, H. Yi, Y. Zhao, S. Song, Quantitative determination of isomorphous substitutions on clay mineral surfaces through AFM imaging: a case of mica, Colloids Surf. A Physicochem. Eng. Asp. 533 (2017) 55–60, https://doi.org/10.1016/j.colsurfa.2017.08.024.
[24] H. Yi, F. Jia, Y. Zhao, W. Wang, S. Song, H. Li, C. Liu, Surface wettability of montmorillonite (0 0 1) surface as affected by surface charge and exchangeable cations: a molecular dynamic study, Appl. Surf. Sci. 459 (2018) 148–154, https://doi.org/10.1016/j.apsusc.2018.07.216.
[25] H. Li, S. Song, X. Dong, F. Min, Y. Zhao, C. Peng, Y. Nahmad, Molecular dynamics study of crystalline swelling of montmorillonite as affected by interlayer cation hydration, JOM 70 (2018) 479–484, https://doi.org/10.1007/s11837-017-2666-2.
[26] C. Peng, F. Min, L. Liu, J. Chen, DFT study of adsorption of water on sodium-montmorillonite (001) basal and (010) edge surface, Appl. Surf. Sci. 387 (2016) 308–316, https://doi.org/10.1016/j.apsusc.2016.06.079.
[27] S. Pirillo, C.R. Luna, I. López-Corral, A. Juan, M.J. Avena, Geometrical and electronic properties of hydrated sodium montmorillonite and tetracycline montmorillonite from DFT calculations, J. Phys. Chem. C. 119 (2015) 16082–16088, https://doi.org/10.1021/acs.jpcc.5b04061.
[28] H. Liu, P. Yuan, D. Liu, H. Bu, H. Song, Z. Qin, H. He, Pyrolysis behaviors of organic matter (OM) with the same alkyl main chain but different functional groups in the presence of clay minerals, Appl. Clay Sci. 153 (2018) 205–216, https://doi.org/10.1016/j.clay.2017.12.028.
[29] M. Liu, Q. Chen, L. Wang, S. Yu, C. Gao, Improving fouling resistance and chlorine stability of aromatic polyamide thin-film composite RO membrane by surface grafting of polyvinyl alcohol (PVA), Desalination 367 (2015) 11–20, https://doi.org/10.1016/j.desal.2015.03.028.
[30] J. Wu, Z. Wang, Y. Wang, W. Yan, J. Wang, S. Wang, Polyvinylamine-grafted polyamide reverse osmosis membrane with improved antifouling property, J. Memb. Sci. 495 (2015) 1–13, https://doi.org/10.1016/j.memsci.2015.08.007.
[31] S. Song, S. Lu, Y. Zhang, A. Lopez-Valdivieso, T. Fort, Aggregation rate of fine particles in turbulent flows, J. Dispers. Sci. Technol. 25 (2004) 67–74, https://doi.org/10.1081/DIS-120027670.
[32] G. Lagaly, S. Ziesmer, Colloid chemistry of clay minerals: the coagulation of montmorillonite dispersions, Adv. Colloid Interface Sci. 100–102 (2003) 105–128, https://doi.org/10.1016/S0001-8686(02)00064-7.